Technical University of Denmark

DTU

Embedded Fibre Bragg Grating Sensor Response Model: Crack Growing Detection in Fibre Reinforced Plastic Materials

Pereira, Gilmar Ferreira; Mikkelsen, Lars Pilgaard; McGugan, Malcolm

DTU Library
Technical Information Center of Denmark

Embedded Fibre Bragg Grating Sensor Response Model: Crack Growing Detection in Fibre Reinforced Plastic Materials

G.Pereira[1], L.P.Mikkelsen[1], M.McGugan[1]

[1]Technical University of Denmark, Department of Wind Energy, Frederiksborgvej 399, 4000 Roskilde

E-mail: gfpe@dtu.dk

Abstract. This article presents a novel method to simulate the sensor output response of a Fibre Bragg Grating (FBG) sensor when embedded in a host material (Composite material or adhesive), during a crack growing/damage event. A finite element model of the crack growth mechanisms was developed, and different fracture modes were addressed. Then an output algorithm was developed to predict the sensor spectrum change during the different stages of the crack growing. Thus, it is possible to identify specific phenomenon that will only happen within the proximity of a crack, as compression field ahead the crack or non-uniform strain, and then identify the presence of such damage in the structure. Experimental tests were conducted in order to validate this concept and support the model. The FBG sensor response model was applied in a delamination of a Wind Turbine trailing edge, to demonstrate the applicability of this technique to more complicated structures, and to be used as a structural health monitoring design tool.

1. Introduction

Fibre Reinforced Plastic materials (FRP or as often called composite materials) have been extensively used in aerospace, automotive, naval, civil engineering and wind energy applications. These FRP materials consist of two macroscopic phases, a stiff fibre phase, usually glass or carbon fibre, and polymeric matrix, usually polyester or epoxy. One of the advantages of fibre reinforced polymer (FRP) composites is that the alignment of the fibres can be arranged to suit the required properties of the intended structure. Taking a wind turbine blade as an example, the requirement for a stiff (but light-weight) structure means fibre orientation primarily along the length of the blade, however in the axial direction this stiff requirement is much lower, meaning that less material is required and used. In this way FRP has the capability to be tailored for a specific application, and a high level of customization of mechanical properties, such as weight-stiffness ration, thermal expansion, chemical/corrosion resistance, fatigue behaviour etc.[1].

However, the increased demand for more cost-effective lightweight composite materials is pushing for advances in material technology, design philosophies and monitoring techniques. An emerging design concept uses the damage tolerance property of FRP materials, where it's capability to hold damage is taken into consideration during the design process. This is achieved by pushing the structure operation limits, and developing models capable of simulating the behaviour of the damaged structure to give a prognosis of the remaining operational life of

the structure. However, accepting the damage and it's unpredictability, requires monitoring technology to track it, by integrated sensors that give information about the presence of damage in an accurate way, it's location and the type of damage [2].

Delamination is one of the most important failure mechanisms in FRP materials and one of the most widespread cause of FRP structures life reduction, this article will focus on this failure mechanism and fibre Bragg gratings as a damage monitoring technique.

2. Delamination in Fibre Reinforced Plastic Materials

Interface fracture by crack growth along interfaces in laminated structures is called delamination, and often is accompanied by the formation of a crack bridging zone, where intact fibres connect the crack faces behind the crack tip, as showed in figure 1. This fibre bridging phenomenon creates an extra obstacle that the crack has to overcome to grow, meaning that the energy required for the crack to grow is higher than that required to initiate it.
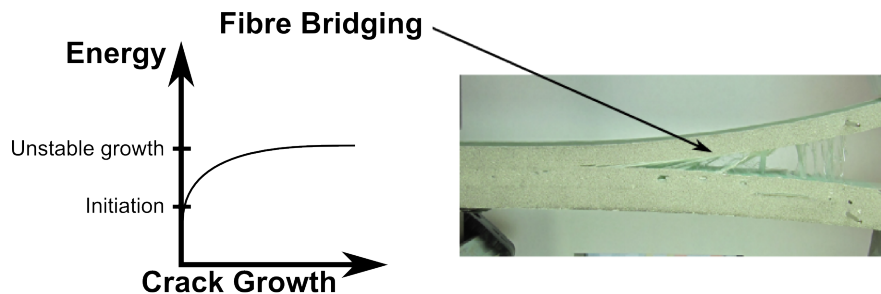
Figure 1. Fibre bridging phenomenon during delamination in a glass fibre specimen.

This large-scale crack bridging zone, can't be handled by linear elastic fracture mechanics. Instead, a cohesive model can be used to describe the fracture process zone. The cohesive law $\sigma_n(\delta_n)$, can be briefly described as a normal traction, σ_n, as function of the normal opening, δ_n in the active cohesive zone [3].

3. Strain Distribution During Crack Growth

To track delamination/crack in FRP materials the sensor/monitoring system selected should be able to track specific fracture features, which only happen in the vicinities of the crack, independent of geometry or loading conditions. To link these fracture features with the measured parameters, the strain distribution around a crack tip during delamination was analysed using Digital Image Correlation (DIC). DIC technique is a non-contact optical method that, by tracking changes in a random pattern on the specimen, can correlate it with deformation/strain of the material.

A pattern was painted on the side surface of the specimen, and ARAMIS^{TM} V6.3 software was used to calculated the strains in each measurement. To perform the measurements, ARAMIS recognizes the surface pattern in the unloaded specimen, and allocates it coordinates in to the image pixels. Then, ARAMIS compares the pattern in the pictures of the loaded specimen, and by tracking the changes calculates the displacement and consequently the strain distribution in the specimen face [4].

To simulate the delamination in a FRP structure, Double Cantilever Beam (DCB) specimens were tested using a fracture testing procedure developed by *Sørensen* [5]. In this testing apparatus the loading is applied through moments and is displacement controlled, which gives a stable crack growth. The DCB specimens were loaded in different conditions at 1mm/min,

ranging pure Mode I to pure Mode II, in order to simulate different crack/delamination situations.

The DCB specimens were manufactured using two FRP material arms, made of unidirectional and triaxial glass fibre layers (SAERTEX UD and TRIAX), with a layup stacking of : $[90/+45/-45/0_4/0_4/+45/-45/90]$, glued by a commercial epoxy structural adhesive (Epikote MGS BPR 135G/Epikote MGS BPH137G). A thin slip foil was placed in the edge of the structural adhesive, to act as a pre-crack and ease crack initiation.

In figure 2 the DCB specimen geometry is presented.
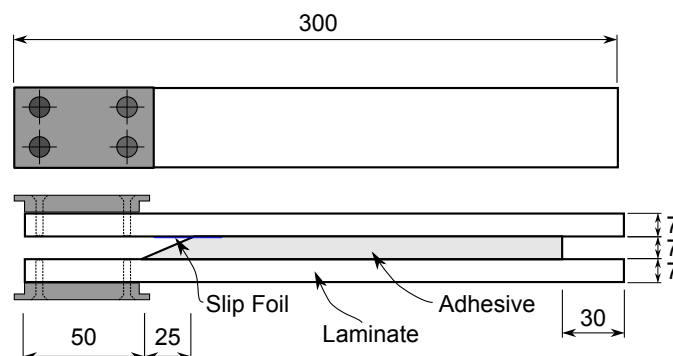
Figure 2. DCB specimen components and geometry.

In figure 3 the strain state at the crack tip during Mode II fracture is shown. We can divide the strain distribution in two distinct contributions: crack tip singularity/material damage and fibre bridging. Near the crack tip, the stress field closely approaches the singular stress field of linear elastic fracture mechanics, meaning that the stress tends to infinity and has a fast variation (high gradient). Also, with the progression of the crack the material/structure losses stiffness increasing the strain, as showed in figure 3a), here it is possible to observe higher values of strain ε_{11} at the crack faces. In the fibre bridging zone ($L < x < 0$), a positive strain ε_{22} was observed, as shown in figure 3c), due to the forces transferred by the fibre that are connecting the two crack faces. These forces are balanced by a compression stress that appears ahead of the crack tip ($x > 0$), which creates a negative strain ε_{22} shown in figure 3c) as a blue area.

4. Crack/Delamination Detection by Embedded Fibre Bragg Gratings

Different sensing technology has been implemented in order to track delamination in FRP materials, such as acoustic emission, vibration/modal analysis, piezo-electric actuators/sensor, strain gages. However, these measurement systems have several limitation in terms of cost, the need of qualified operators and impracticability to be used under operation.

Fibre Bragg Gratings (FBG) are a very a promising technology to track the presence of delamination/cracks in an operational FRP structure, due to their capability to be embedded in the material, without compromising the structural resistance. The FBG small size, 125 μm of diameter, makes it virtually non-intrusive to the material. FBG sensors, also have other interesting features, such high resolution, multiplexing capability, immunity to electromagnetic fields, chemical inertness and long term stability (fatigue behaviour). A Fibre Bragg Grating is formed when a permanent periodic modulation of the refractive index is induced along a section of an optical fibre, by exposing the optical fibre to an interference pattern of intense ultra-violet light [2]. The photosensitivity of the silica exposed to the ultra-violet light is increased, so when the optical fibre is illuminated by a broadband light source, the grating diffractive properties are such that only a very narrow wavelength band is reflected back. When any external phenomenon

**Figure 3.** Strain distribution at the crack tip during Mode II fracture.
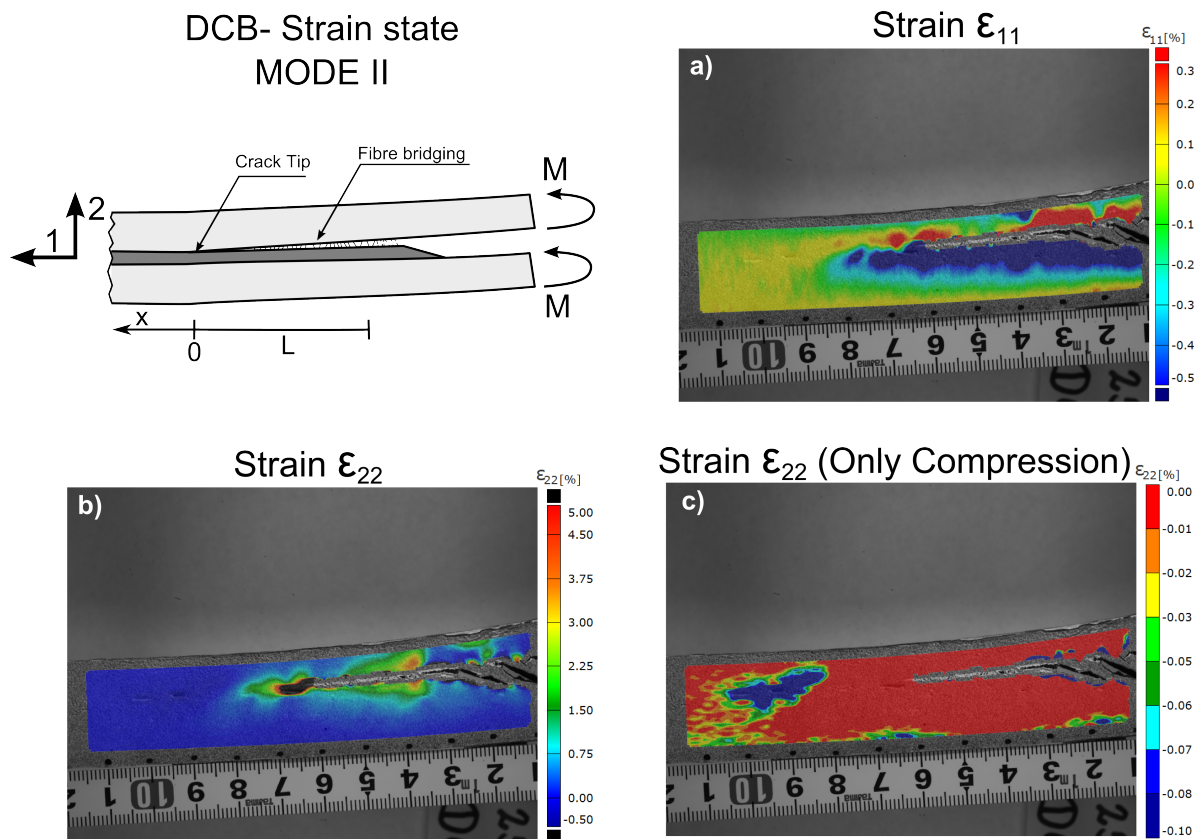
creates a change in the grating, like temperature, strain, compression, non-uniform strain fields, etc. this will create a change in the reflected light.

As discussed in section 3, during a crack/delamination event different fracture features will be present near the crack tip. Being able to identify and measure this specific phenomena with a FBG sensor is the key factor to correctly determining the presence of damage and it's growth.

In figure 4, the different stages of the FBG responses under a crack growth event are presented. First, before the crack reaches the proximity of the grating, figure 4a), the material will build up uniform strain, that will make a uniform wavelength shift in the FBG reflected peak. Next, a compression field is formed ahead of the crack tip due to the formation of a crack bridging zone, as showed in figure 3c), when it reaches the grating area it creates a peak splitting of the FGB response, figure 4b). Then, when the grating is near the influence of the crack singularity, as discused in section 3 and presented in figure 3a), a non-uniform strain field will also modify the shape of the reflected peak, as showed in figure 4c). Finally, after the crack passes the FBG sensor, the shape of the reflected peak will go back to the original shape, and the sensor response will again be a simple wavelength shift, because at this stage only uniform strains will be present at the FBG, figure 4d).

4.1. Response to Uniform Strain

The wavelength shift $\Delta\lambda_b$ represented in figure 4a), of an embedded FBG under a uniform variation of strain ϵ_{xx}, along the fibre direction, and considering no temperature variation (during crack growth temperature variation is neglected), is given by the equation 1,
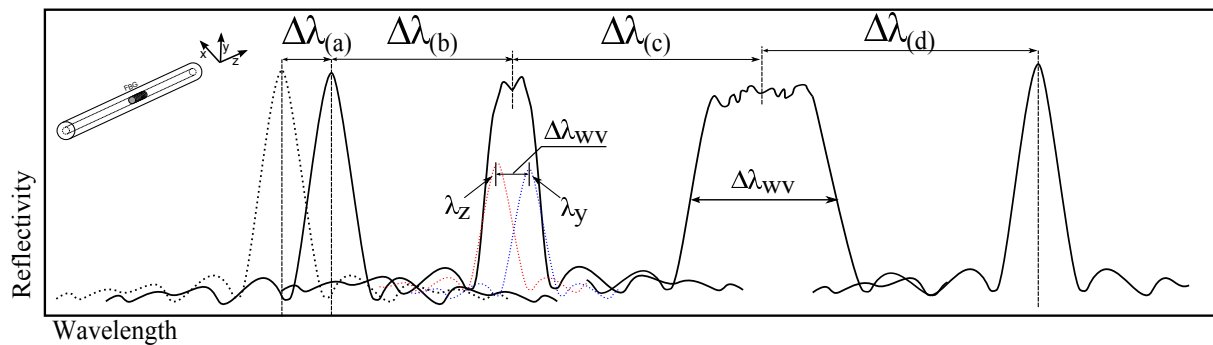
Figure 4. Different stages of the FBG response under a crack growth event.

$$\frac{\Delta\lambda_b}{\lambda_b} = (1 - p_e)\varepsilon_{xx} \qquad (1)$$

where p_e is a photoelastic coefficient [6].

4.2. Response to Transverse Force

An optical fibre can present a birefringent behaviour, defined by the change of the refractive index n_{eff} in the two directions n_{effy} and n_{effz}, when the grating is subjected to a transverse force [7, 8, 9, 10]. The increase in the width of the reflected peak represented in figure 4b), is given by the equation 2,

$$\Delta\lambda_{WV} = 2\Lambda|\Delta n_{effz} - \Delta n_{effy}| = \frac{\Lambda n_o^3}{E_f}[(1 + \nu_f)p_{12} - (1 + \nu_f)p_{11}]|\sigma_z - \sigma_y| \qquad (2)$$

where $\sigma_{y,x}$ is the transverse stress, E_f is the elastic modulus of the optical fibre, ν_f is the Poisson's ration, n_0 is the initial refractive index, p_{11} and p_{12} are the photo-elastic coefficients of the optical fibre.

4.3. Response to Non-Uniform Strain

As demonstrated by Peters [11], in a uniform grating the applied strain will induce a change in both grating period and the mean index. These two effects can be superimposed by applying an effective strain of "$(1 - p_e)\varepsilon_{xx}(x)$". Then it is possible to rewrite the grating period as:

$$\Lambda(z) = \Lambda_0[1 + (1 - pe) \times \varepsilon_{xx}(x)] \qquad (3)$$

where Λ_0 is the grating period with zero strain. The non-uniform strain effect can be approximated by using the maximum and minimum strain values along the grating. So, the maximum grating period Λ_{max} and minimum Λ_{min} can be calculated using the equation (3). Thus, an approximated increase of the width of the reflected peak due to a non-uniform strain $\Delta\lambda_{IW}$ is given by the equation 4:

$$\Delta\lambda_{WV} = 2n_{eff}\Lambda_{max} - 2n_{eff}\Lambda_{min} \qquad (4)$$

5. Finite Element Method Model of the FBG response: Crack Detection Model

The major goal of this study was to developed a numerical model to predict the FBG output in a general crack growth situation. This sensor-damage-structure model provides a tool to study the application of this monitoring technique in other locations, by predicting the sensor

output and deciding, based on this, the best sensor-structure configuration. To accomplish this, an algorithm was developed, using the measurement principals/variables and equations developed in section 3 and 4. This algorithm was incorporated in to the FEM Model, using *Python* programming language.

Table 1. Material Properties used in the DCB Model

Composite Material		Interface (Cohesive Law)			Adhesive
Triaxial Fabric (Composite)	Uniaxial Fabric (Composite)	Elastic	Damage (Quadratic Stress	Damage Evolution	Elastic
$E_1 = 44.3$ GPa; $E_2 = E_3 = 12.9$ GPa; $\nu_{12} = \nu_{13} = \nu_{13} = 0.23$; $G_{12} = G_{13} = G_{23} = 4.4$ GPa	$E_1 = 23.8$ GPa; $E_2 = E_3 = 15.05$ GPa; $\nu_{12} = \nu_{13} = \nu_{13} = 0.513$; $G_{12} = G_{13} = G_{23} = 4.4$ GPa	K= 4.2 E12 Pa;	$\sigma_n = 2.64$ MPa; $\sigma_t = 22.15$MPa	$\delta_n = 1.4$; $\delta_t = 0.37$;	E= 4.56 GPa; $\nu = 0.35$

As a study case, the delamination in the trailing edge of a wind turbine blade was addressed, based on a real trailing edge configuration used by the *DTU 10 MW Reference Wind Turbine* [12]. The trailing edge was modelled as a 2D and 3D Double Cantilever Beam, where different loading conditions (ranging pure Mode I to pure Mode II fracture modes) simulate the different fracture cases that can occur in this structure. The crack growth in the DCB specimens was modeled using cohesive elements, which describe the cohesive law that governs the crack growth mechanism. The geometry of the DCB specimen is the same as used in figure 2 and section 3, and the material properties used in the model are presented in the table 1.
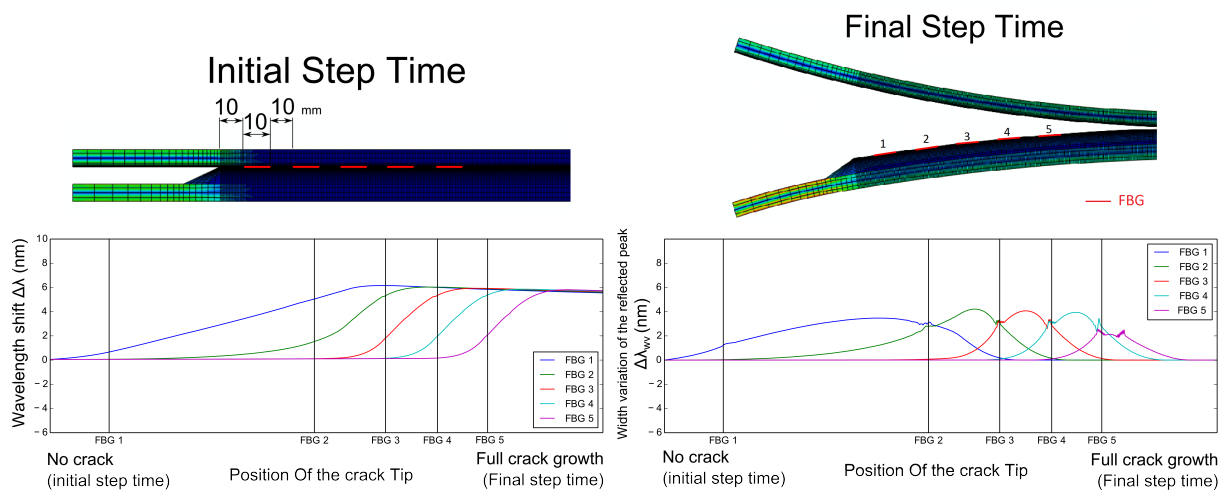

Figure 5. FEM model Sensor output for Mode I loading case.

### 5.1. Model Experimental Validation

DCB specimens with the same material-sensor configuration as the model, were tested following the procedure described in section 3. The DCB specimens were instrumented with an array of FBG sensors embedded in the host material. A good agreement between the finite element model and the experiments was found. The FEM was able to represent the crack growth under different loading cases, and the sensor output model matched the experiments, showing the expected sensor response to fracture phenomena, already measured by DIC technique and described in section 3.
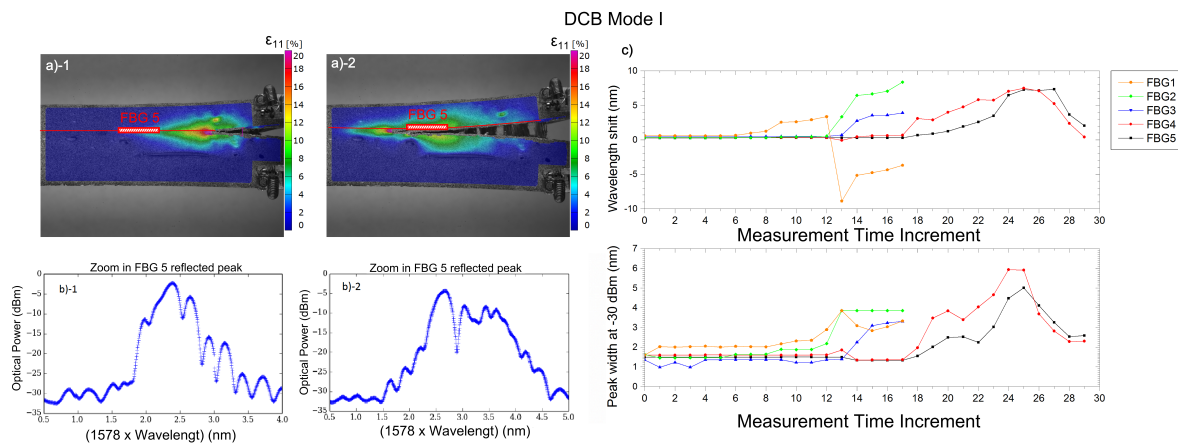
Figure 6. Model Experimental Validation for a Mode I loading case. a) Digital Image Correlation technique: Longitudinal strain ε_{11}, b) FBG 5 reflected peak, c) FBG sensor response during crack growth.

6. Application of the Model
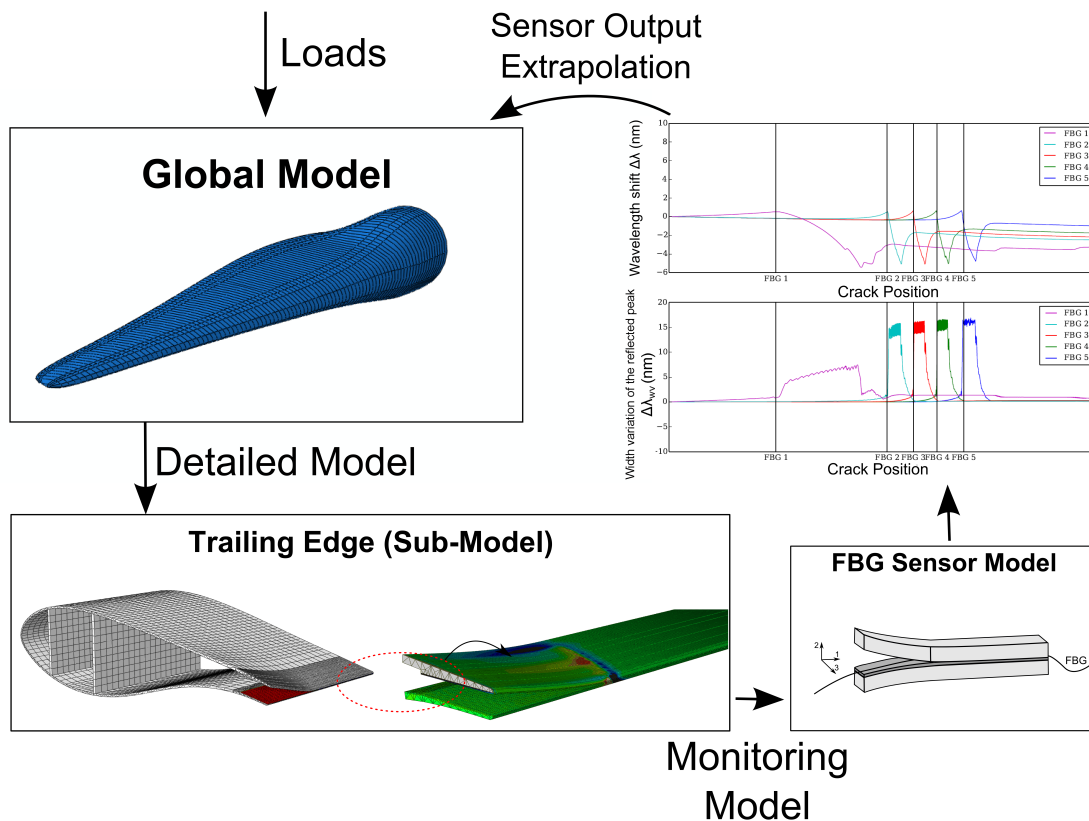
Figure 7. FBG sensor output simulation: Crack detection in Wind turbine trailing edge.

The FBG response model was applied in to a "full" Wind turbine blade model to predict the sensor output during failure of the trailing edge, as schematic represented in figure 7. To address

this, a sub-model of the blade containing a detailed trailing edge geometry was modelled using the loads given by the global model. Then the FBG-Output model was applied and the results extrapolated to the full structure model.

7. Conclusion

In this article the capability of Fibre Bragg Gratings embedded in composite material to detect and track cracks/delamination was demonstrated. The use of the digital image correlation technique proved that specific fracture features near the crack can create a change in the shape of the reflected peak. Thus, it is possible to extract information from the sensor that is independent of the loading type, geometry and boundary conditions, and depends only on the proximity of the crack. This fact allows the application of this technique in general composite material structures.

The prediction of the sensor response by the FEM model makes it possible to study the application of this monitoring technique in other locations, predict the sensor output, and decide the best sensor-structure configuration. This "FBG output model" concept can have an impact in condition monitoring methodology and maintenance, by optimising the measurement by sensors, enabling more diverse and accurate damage detection, giving better characterization of the damage (type and size), and giving information for prediction of the residual structural life, and if possible, repair.

8. Acknowledgement

References

[1] Jones R 1999 *Mechanics of composite materials* (Taylor & Francis) ISBN 156032712x, 9781560327127
[2] McGugan M, Pereira G, Srensen B, Toftegaard H and Branner K 2015 *Royal Society of London. Philosophical Transactions A. Mathematical, Physical and Engineering Sciences* **373** ISSN 1364-503X
[3] Sørensen B 2010 *Cohesive laws for assessment of materials failure:Theory, experimental methods and application* Ph.D. thesis
[4] ARAMIS™ 2011 *User Manual. Version 6.3, GOM optical measuring Techniques, Mittelweg 7-8, D-38106 Braunschweig, Germany* (Germany)
[5] Sørensen B F, Jørgensen K, Jacobsen T K and Østergaard R C 2006 *International Journal of Fracture* **141** 163–176 ISSN 0376-9429
[6] Morey W, Meltz G and Glenn W 1990 *OE/FIBERS'89*
[7] Sørensen L, Botsis J, Gmür T and Humbert L 2008 *Composites Science and Technology* **68** 2350–2358 ISSN 02663538
[8] Zhang W, Chen W, Shu Y, Lei X and Liu X 2014 *Applied Optics* **53** 885 ISSN 0003-6935
[9] Jülich F and Roths J 2010 **7726** 77261N–77261N–9
[10] Bosia F, Giaccari P, Botsis J, Facchini M and Limberger H G 2003 *Smart Materials and Structures* **925** 925–934
[11] Peters K, Studer M, Botsis J, Iocco A, Limberger H and Salath R 19–28
[12] Bak C, Zahle F, Bitsche R, Kim T, Yde A, Henriksen L, Hansen M, Blasques J, Gaunaa M and Natarajan A 2013 The dtu 10-mw reference wind turbine URL `http://dtu-10mw-rwt.vindenergi.dtu.dk/`